Robotica (2022), **40**, pp. 2996–3012
doi:10.1017/S0263574722000029

CAMBRIDGE
UNIVERSITY PRESS

RESEARCH ARTICLE

Control of flexible knee joint exoskeleton robot based on dynamic model

Biao Liu, YouWei Liu, Zikang Zhou and Longhan Xie*

Shien-Ming Wu School of Intelligent Engineering, South China University of Technology, Guangzhou, 510640, China
*Corresponding author. E-mail: melhxie@scut.edu.cn

Received: 26 October 2021; **Revised:** 8 December 2021; **Accepted:** 1 January 2022; **First published online:** 3 February 2022

Index Terms: Rehabilitation, Poststroke, Exoskeleton robot, Bowden Cable

Summary

The knee joint plays a significant role in ground clearness, which is a crucial subtask of normal walking and avoiding falls. While post-stroke survivors are often faced with muscle weakness during walking, which leads to inadequate knee flexion. The lack of ground clearance caused by inadequate knee flexion will severely impede walking, increase metabolic exertion, and increase the risk of falls. A compliant exoskeleton robot possesses more favorable edges than other rigid ones in lightweight, safety, sense of comfort, and so on. We developed a new type of soft exoskeleton robot to assist the knee joint to achieve desired movements with Bowden cable transmitting force and torque. With the agonist–antagonist driving method, like a group of muscles working, we have explored dual-motors structure to realize the knee flexion function. It has built a standard dynamic model to analyze stability and realize the control law. We have conducted simulation and prototype experiments to verify the feasibility and usefulness of our method. The results show that the device can compensate for the lack of the knee joint driving force and realize the reference movement. Finally, we concluded that our method is a desirable way, and the scheme could improve the knee flexion ability and clearing ground.

1. Introduction

In recent years, stroke has become the top ten deadly diseases that cause death in China [1]. Most of the survivors after stroke require rehabilitation to regain basic function after a stroke. Restoration of lower limb function is important to ensure the quality of daily life and participation in community life. Recovering the paretic knee joint has a crucial significance in clearness ground and avoiding falls during the swing phase of the gait cycle in walking.

A stiff-knee gait is a common post-stroke gait typically characterized by inadequate knee flexion during the swing phase [2]. This leads to asymmetry in walking and increased energy consumption. It can also severely impair the ability to clear the ground and increase the risk of falls. Moreover, with the advent of an aging population, an increasing number of elderly people are facing the problem of muscle weakness. Muscle weakness in the lower extremities will lead to a decline in independent mobility or the ability to perform daily living activities in the community [3, 4]. In walking, the knee joint plays a very important role in supporting weight (supporting phase) and clearing the ground (swing phase), and the mobility of the knee joint determines the ability to walk properly and safely. Therefore, it would be very significant to assist walking through the knee joint exoskeleton. Second, the knee joint motion is driven by the lightweight and flexible Bowden cable, which will greatly avoid the disadvantage of high rotation inertia and load effect caused by the traditional rigid exoskeleton linkages. According to a related research, the metabolic cost of carrying a 10% body weight payload at thigh and shank was about to increase for 20% [5]. At the same time, the flexible Bowden cable agonistic–antagonistic muscle-like driving structure can avoid joint alignment problems.

© The Author(s), 2022. Published by Cambridge University Press.

https://doi.org/10.1017/S0263574722000029 Published online by Cambridge University Press

Compared to this novelty driving way, traditional rigid knee exoskeleton faces redundant mechanisms, high inertia, and mismatch between biological and mechanical joints. Recent flexible Bowden cable-based actuation offers a viable idea for building lightweight knee assistive devices. Especially, there are plenty of applications in bionic robots [6], neurosurgical robots [7], rehabilitation robots [8–10], and function augmentation robots [11, 12], which used the Bowden cable to implement these devices and functions [13, 14].

Recently, the Bowden cable-driven exoskeletons have attracted many researchers' attention. Hence, several studies have been done in the robot field, surgical devices, and remote manipulating devices. Thompson, et al. [15] combined the pneumatic actuators and Bowden cable to develop a novel augmenting shoulder flexion exoskeleton, but they only considered the static situation while the movement of the body is always dynamic. Some applications aim at augmenting the strength of part of joints, such as hip and ankle joints. However, most of them only achieve a part of a degree of freedom (DoF) or part stroke of a movement cycle and only focus on the pulse force output with proportion integration differentiation (PID) controller [12, 16, 17], which key parameters depend on the experience and without strict proof of stability theory. Also, the control way only depending on the errors need more energy consumed. In application, this may also need more exercise to adaptive the strong pulse force acting on the body. Some studies also concentrated on body function augmentation. And they achieved a considerable breakthrough as well. However, they have not constructed an exact model, and the improvements have a high dependency on individuals and experience [10, 18–20]. Because the driving force and torque were transmitted by Bowden cables, which include a sea of variances, and the control method of the precise output is a challenging task. Jeong, et al. [21] utilized the extra sensor combined with Bowden cable to improve the hysteresis problem. They reduce the control error of the driving force from 4.22N to 0.69N. But the Bowden cable with special sensors must be costumed and the cost is not under control. Jhon et al. [22] has developed a cable-driven device, called CUBE, for upper limbs rehabilitation at home. A novel end-effector combined with autotuning algorithm and vision-based control has been utilized for assisting the forearm moving. But these end-effector devices only focus on the space of task, ignoring the joint movement space. This may increase the risk of joint injury.

In this paper, we proposed a new method that can help joint in the whole stroke with complete DoF in its joint working space. The dual-motors structure, driven by Bowden cable, has been developed to assist the biotic knee joint. More feasibility and torque can be offered with the cooperation between two motors. It adopted the bionic structure mimicking the muscles attached to bones with Bowden cable, which could avoid the joint misalignment problem. A standard dynamic system control model was used to achieve the desired performance. Both simulation and experiments were carried on to prove the correction and feasibility.

2. Methodology

Most individuals who suffered a stroke and lost part of their locomotion function need rehabilitation to improve their mobility to enhance the quality of life and community participation.

Exoskeletons, as a workable option, offer a favorable and expectational way to help the patients to recover. The repeatable movement tasks of limbs are very suitable for exoskeleton robots' working mode. And this will boost the efficiency of rehabilitation and low the cost of post-stroke treatment.

By analyzing the anatomy of knee joint movement, the dynamic model of the knee combined with the wearing exoskeleton has been built up. Then, the corresponding control law has been designed according to the dynamic model and Lyapunov stability theory.

2.1. Anatomy of the knee joint

The knee joint is a very important joint in the body. Not only does it provide support for the body to resist gravity but it also has to generate flexion and extension for many forms of human locomotion.

https://doi.org/10.1017/S0263574722000029 Published online by Cambridge University Press

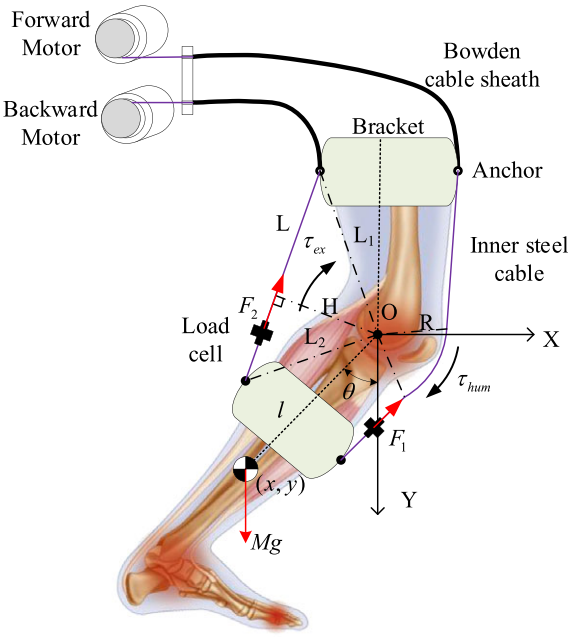


Figure 1. *The knee joint exoskeleton robot diving the shank.*

According to anatomy of knee, the movement in the sagittal plane mainly depends on its agonistic and antagonistic muscle groups. The extension mainly originates from the agonistic muscle group that includes quadriceps femoris muscle group. The flexion arises from the antagonistic muscle group that consists of the hamstrings. The agonist muscle group is approximately three times stronger than the antagonist muscle group due to the continuous contraction to resist gravity and provide negative acceleration for stopping flexion [23].

However, patients with stroke or spinal injuries often fail to obtain a normal gait due to abnormal knee motion. The knee cannot flex and extend properly, resulting in the affected side not clearing the road well in the swing phase. This could greatly increase the risk of falling to the ground. Therefore, it is important to better assist the knee joint to complete knee flexion and extension movements to help patients walk normally. It is important to reduce the chance of secondary injury in a fall.

In this paper, we proposed a knee exoskeleton with Bowden cable to assist the knee joint based on the form of agonist–antagonist muscle groups acting on human joints. The contraction of the Bowden inner cable relative to the outer sheath simulates the mechanism of muscle generation of motion, and the knee joint is assisted by a lightweight wearable structure without introducing a new additional mechanical joint, as shown in Fig. 1. This design without additional rigid joints will reduce joint constraints and reduce the risk of injury.

2.2. Dynamic model of the control system

The dynamic model always represents the relationship between movement parameters like position, velocity, acceleration, and force parameters, including all kinds of force and torque. Specifically, taking the human body as an example, the movement parameters include not only joint angle but also the displacement of the center of mass (CoM) of shank and foot and their corresponding speed and acceleration. Of course, joint force and torque that come from muscle contractions produce the corresponding movement of the body, like walking, jogging, jumping, and so on. Hence, it is very imperative to generate highly precise motion and path via this kind of dynamic model.

https://doi.org/10.1017/S0263574722000029 Published online by Cambridge University Press

There are several methods to build the dynamic model, such as the Newton –Euler method [24], Kane method [25], Lagrange method [26], and so forth. As for complex multirigid modeling, the Lagrange method has a uniform form and appeals to plenty of researchers.

In this paper, the shank-foot and the worn exoskeleton are assumed to be rigid linkages. Then they all rotated around the knee joints. Because of mimicking and assisting the knee flexion motion, the thigh has been fixed in the vertical direction, as shown in Fig. 1. Then dynamic model has been derived according to the Lagrange method as follows.

According to the Lagrange method and Fig. 1, the CoM position of the shank is described as (x, y)

$$\begin{cases} x = -l\sin\theta \\ y = \ l\cos\theta \end{cases} \tag{1}$$

where l is the length from origin to CoM of the shank, and θ means the knee joint angle. Next, taking the derivative of the position regarding time, we got the velocity of CoM:

$$\begin{cases} \dot{x} = -l\cos\theta\dot{\theta} \\ \dot{y} = \ -l\sin\theta\dot{\theta} \end{cases} \tag{2}$$

where $\dot{\theta}$ represents the angular speed. Then kinetic energy of the system V can be described as

$$\begin{aligned} V &= V_m + V_r \\ &= \frac{1}{2}M(\dot{x}^2 + \dot{y}^2) + \frac{1}{2}I\dot{\theta}^2 \\ &= \frac{2}{3}Ml^2\dot{\theta}^2 \end{aligned} \tag{3}$$

where V_m and V_r are translational energy and rotational energy, respectively. M is the total mass of shank, I is the moment of inertia of shank, and $I = \frac{1}{3}Ml^2$.

Considering $\theta = 0$ as the reference posture (the thigh is vertical), the potential energy of the system can be defined as follows:

$$E = Mgl(1 - \cos(\theta)) \tag{4}$$

Hence, the Lagrange function can be expressed as follows:

$$L = V - E \tag{5}$$

$$\frac{d}{dt}\left(\frac{\partial L}{\partial\dot{\theta}}\right) - \frac{\partial L}{\partial\theta} = \tau \tag{6}$$

$$\frac{4Ml^2}{3}\ddot{\theta} - Mgl\sin(\theta) = \tau \tag{7}$$

It also can be written as follows:

$$\ddot{\theta} - \frac{3g}{4l}\sin(\theta) = \frac{3}{4Ml^2}\tau \tag{8}$$

where τ represents the whole driving torque, including muscles producing torque τ_{hum} and motors generating torque τ_{ex}.

$$\tau = \tau_{hum} + \tau_{ex} \tag{9}$$

2.3. The design of controller

The ideal model of the system was expressed as Eq. (7); however, the actual situation is always more complex. There are other factors that may exert a certain influence on the performance of the system. One of the most important factors among these is the joint viscous damping coefficient B. So, the ideal

https://doi.org/10.1017/S0263574722000029 Published online by Cambridge University Press

model can be changed to

$$\frac{4Ml^2}{3}\ddot{\theta} + B\dot{\theta} - Mgl\sin(\theta) = \tau \tag{9}$$

The next step was to design the controller to track the reference trajectory. We redefined the variances:

$$\begin{cases} z_1 = \theta \\ z_2 = \dot{\theta} = \dot{z}_1 \\ u = \tau \end{cases} \tag{10}$$

The goal of the controller was to trace the reference input, so the object of the controller can be described as

$$\theta \to \theta_d \text{ or } z_1 \to z_{1d} \tag{11}$$

where θ_d and z_{1d} are the desired variance. Then the traced error and derivative of error can be defined as

$$e = z_{1d} - z_1 \tag{12}$$

$$\dot{e} = \dot{z}_{1d} - \dot{z}_1 \tag{13}$$

Of course, we hope the traced error was closed to zero, which means the reference trajectory is traced precisely. Next, according to the second Lyapunov method, we defined positive definite energy function $V_1(e)$:

$$V_1(e) = \frac{1}{2}e^2 \tag{14}$$

Derivative of $V_1(e)$ with respect to time:

$$\begin{aligned} \dot{V}_1(e) &= e\dot{e} \\ &= e(\dot{z}_{1d} - \dot{z}_1) \\ &= e(\dot{z}_{1d} - z_2) \end{aligned} \tag{15}$$

In order to get a stable system, it must subject to $\dot{V}_1(e) < 0$, merely negative definite. So, let:

$$\dot{z}_{1d} - z_2 = -k_1 e, \quad \forall k_1 > 0 \tag{16}$$

where k_1 is the control parameter, to get desired z_{2d}, let

$$z_{2d} = \dot{z}_{1d} + k_1 e \tag{17}$$

The system can maintain stable and the error is enough small. Similarly, we seek a new goal:

$$z_2 \to z_{2d} \tag{18}$$

And the new error was defined as

$$\delta = z_{2d} - z_2 \tag{19}$$

$$\dot{\delta} = \dot{z}_{2d} - \dot{z}_2 \tag{20}$$

Eq. (9) (17)(10) substituted into Eq. (20):

$$\begin{aligned} \dot{\delta} &= \dot{z}_{1d} + k_1 e + \frac{3B}{4Ml^2}z_2 - \frac{3g}{4l}\sin(z_1) - \frac{3}{4Ml^2}u \\ &= \ddot{z}_{1d} + k_1(\dot{z}_{1d} - z_2) + \frac{3B}{4Ml^2}z_2 - \frac{3g}{4l}\sin(z_1) - \frac{3}{4Ml^2}u \end{aligned} \tag{21}$$

To let error close to zero, we redefined the positive definite energy function $V_2(e, \delta)$:

$$V_2(e, \delta) = V_1(e) + \frac{1}{2}\delta^2 \tag{22}$$

https://doi.org/10.1017/S0263574722000029 Published online by Cambridge University Press

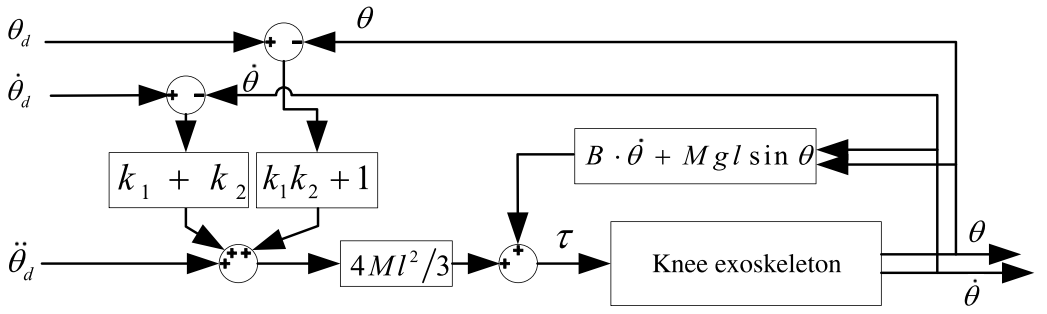


Figure 2. *The control scheme of the knee exoskeleton.*

Derivative of $V_2(e, \delta)$ with respect to time:

$$\begin{aligned}\dot{V}_2(e,\delta) &= \dot{V}_1(e) + \delta\dot{\delta} \\ &= e(\dot{z}_{1d} - (z_{2d} - \delta)) + \delta\dot{\delta} \\ &= e(\dot{z}_{1d} - z_{2d}) + \delta(e + \dot{\delta}) \\ &= -k_1 e^2 + \delta(e + \dot{\delta})\end{aligned} \tag{23}$$

When $\dot{V}_2(e, \delta) < 0$ at balance, the system shows asymptotic stability. And this can make sure that the error approaches zero. Only need Eq. (23) subject to:

$$e + \dot{\delta} = -k_2\delta, \quad \forall k_2 > 0 \tag{24}$$

Let Eq. (24) substitute into Eq. (21):

$$\begin{aligned}&e + \ddot{z}_{1d} + k_1(\dot{z}_{1d} - z_2) + \frac{3B}{4Ml^2}z_2 \\ &\quad - \frac{3g}{4l}\sin(z_1) - \frac{3}{4Ml^2}u = -k_2\delta\end{aligned} \tag{25}$$

Eq. (12)(19)(20) substituted Eq. (25):

$$\begin{aligned}u &= \frac{4Ml^2}{3}(e + \ddot{z}_{1d} + k_1(\dot{z}_{1d} - z_2) + \frac{3B}{4Ml^2}z_2 \\ &\quad - \frac{3g}{4l}\sin(z_1) + k_2\delta) \\ &= \frac{4Ml^2}{3}(z_{1d} - z_1 + \ddot{z}_{1d} + k_1(\dot{z}_{1d} - z_2) + \frac{3B}{4Ml^2}z_2 \\ &\quad - \frac{3g}{4l}\sin(z_1) + k_2((\dot{z}_{1d} + k_1(z_{1d} - z_1)) - z_2))\end{aligned} \tag{26}$$

Finally, we replace the variance with angular parameters:

$$\begin{aligned}\tau = &\frac{4Ml^2}{3}(\theta_d - \theta + \ddot{\theta}_d + k_1(\dot{\theta}_d - \dot{\theta}) + \frac{3B}{4Ml^2}\cdot \\ &- \frac{3g}{4l}\sin(\theta) + k_2((\dot{\theta}_d + k_1(\theta_d - \theta)) - \dot{\theta}))\end{aligned} \tag{27}$$

where θ_d, $\dot{\theta}_d$, and $\ddot{\theta}_d$ are the reference angular position, angular speed, and angular acceleration, respectively. The control torque can be represented as Fig. 2.

https://doi.org/10.1017/S0263574722000029 Published online by Cambridge University Press

2.4. Output torque of the actuator

The extern torque comes from the motor acting on the knee joints by Bowden cable. The sum torque was the combined result of bilateral agonist–antagonist tension. So, the cooperation control of the two motors is the key factor to generator desired torque acting on the joints.

As shown in Fig. 1. We recorded the initial angle between the thigh L_1 and shank L_2 as φ_0 when the θ is zero, according to the definition of torque:

$$\tau_{ex} = F_2 \cdot H - F_1 \cdot R \tag{28}$$

where F_1 and F_2 are the tensions generated by two motors driving Bowden cables contraction, respectively. H and R are their responding force arm. R is the knee joint's equivalent radius and can be measured in anthropometry. H can be calculated as

$$H = \frac{L_1 L_2 \sin(\varphi_0 - \theta)}{\sqrt{L_1^2 + L_2^2 - 2L_1 L_2 \cos(\varphi_0 - \theta)}} \tag{29}$$

where L_1 and L_2 are structural parameters shown in Fig. 1.

The shank-foot movements are always a combination of work from joint muscles and exoskeleton robots. While there is some special condition that the subject in the passive condition. Their muscles cannot offer any force to drive their body to finish the desired movement, just like early stroke patients in complete myasthenia ($\tau_{hum} = 0$) or in the passive rehabilitation mode. Considering these situations, the external force and torque can help them achieve their goal. And the relationship of F_1, F_2 and their force arms determines what movement can be achieved:

1) $\tau_{ex} > 0$, knee flexion;
2) $\tau_{ex} < 0$, knee extension;
3) $\tau_{ex} = 0$, maintaining the posture.

When exerting force to the Bowden cable, the two motors connected to the Bowden cable are designed in consistent with knee joint movement. The active cable tensor can be calculated according to Eq. (28) and wanted joints torque τ_{ex}.

3. Simulation and Experiments

To demonstrate the feasibility and efficiency of our proposed method above, some experiments have been carried out both in simulation and in prototype.

3.1. Parameter tuned

Before simulation and experiments, some parameters concerned with the human body need to be determined. According to related researches about biomechanics [27–29], almost all body parameters, say a mass of body segments, length, and so forth, are subjected to certain functions with their whole body mass and height.

According to anthropometric data, the mass of the leg (not including the tight) and foot is 6.1% of the whole-body mass. And the mass is at 60.6% of the leg and foot's length (Femoral condyles are the proximal end). The shank and foot total weight can be supposed as 8 kg, and the length as 0.5 m. The damper of the joint is set to a series value from 0.1 to 0.8.

As for the real experiments, it is essential to measure the real values before the experiments start. For the sake of uniformity, we set the simulation parameters and the real experiment parameters to be the same. In all, the setting of all the parameters is shown in Table I.

https://doi.org/10.1017/S0263574722000029 Published online by Cambridge University Press

Table I. *Parameter setting.*

Name	Value	Units
M	8.0	kg
l	0.25	m
φ_0	1.92	rad
B	0.1,0.3,0.5,0.8	N·s/m
L_1	0.13	m
L_2	0.20	m
k_1	100	/
k_2	100	/

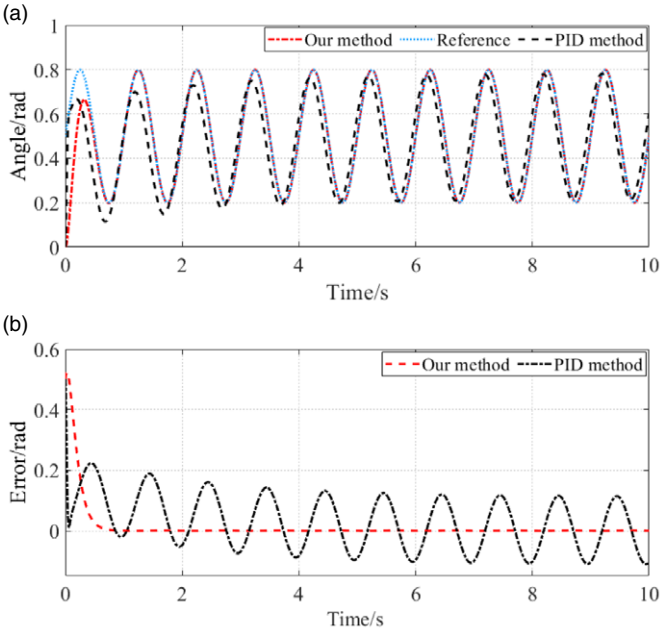


Figure 3. *(a) Is the results of the control system tracing the sinusoid curve, there are two method results that follow the desired path: one is our method, and the other one is the traditional PID method. They all have a nice performance; (b) is the tracing error, with the viewpoint of error, our method has the better following capability.*

3.2. Simulation

Simulation is always a highly effective approach to verify the validity of some algorithm, or control system. Here, we simulate the control system to trace two different desired trajectories in the MATLAB 2019b. One test trajectory is a continuous sinusoidal signal with a frequency of 0.5 Hz. And the other is a step-wise signal with 4 s. The general PID method was also be tested as a comparison.

There is an obvious improvement when the control system follows the continuously changing joint angle (shown in Fig. 3 a). The trace error quickly approaches zero within a second. However, the traditional PID method is slower, and there is some error finally within test time, as shown in Fig. 3 (b). As for the step-wise reference path, though two kinds of methods exist some error because of the sharply changing (shown in Fig. 4 (a). They all can follow the path roughly, as shown in Fig. 4 (a).

https://doi.org/10.1017/S0263574722000029 Published online by Cambridge University Press

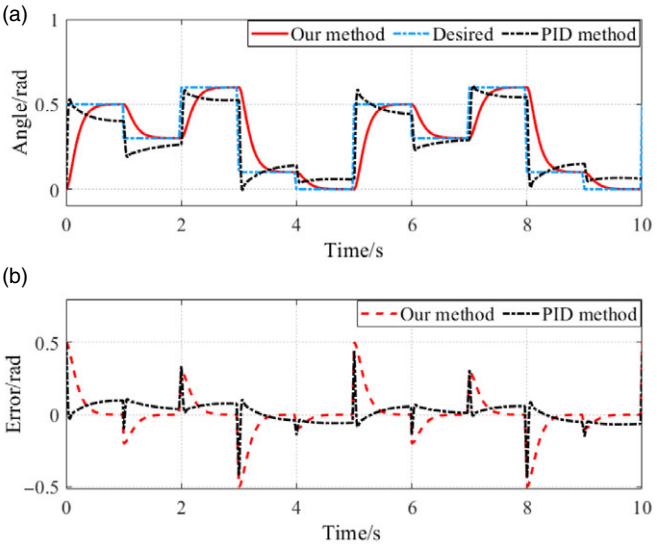


Figure 4. *(a) Is the results of the control system tracing the step-wise curve, there are two method results that follow the desired path: one is our method, and the other one is the traditional PID method. They all have a nice performance; (b) is the tracing error, with the viewpoint of error, both of them have some error when following the desired step-wise curve.*

3.3. Experimental test bench

To validate the feasibility of the proposed control scheme, a test bench that includes a wearable knee joint exoskeleton (as shown in Fig. 5), controller PC, and sensor subsystem have been built. The exoskeleton has been worn on a customized mannequin.

3.3.1. Flexible Bowden cable driving

To assist in the rehabilitation of post-stroke folks, we have developed a new knee joint soft exoskeleton based on Bowden cable transmitting driving force and torque. With the Bowden cable connected to the driving motors and the actuators, it is possible to realize the feasibility and softness when the robot is attached to the body. This scheme of hardware system composition brings a series of advantages. The three prime merits can be summarized:

- The segregation between driving sources and actuators with Bowden cable can minimize the rotational inertia, which boosts the work efficiency;
- Having not rigid joints and linkages attached to the human body, it could avoid the parasitic constraints and limitations affecting body movement;
- Soft characteristic of Bowden cable removing of the problem of joint axis alignment problem, which avoids chafe and hurting. It also may provide a sense of comfort and safety for the user.

Hence, the Bowden cable is a desirable approach to build the knee rehabilitation exoskeleton, whose driving sources are placed on the surrounding frame. The flexible and slender properties make the wearing part of the exoskeleton lightweight and compact possible, which can reduce the load effect on the user.

The type of Bowden cable is also a key factor that affects the performance of the system. Similarly, some parameters need to be selected according to applications. In our system, the most three characteristics are friction coefficient, the ability to bend, and physical size. The less friction, the less energy loss, and the high efficiency. Reducing friction not only benefits energy transmission but also improves

https://doi.org/10.1017/S0263574722000029 Published online by Cambridge University Press

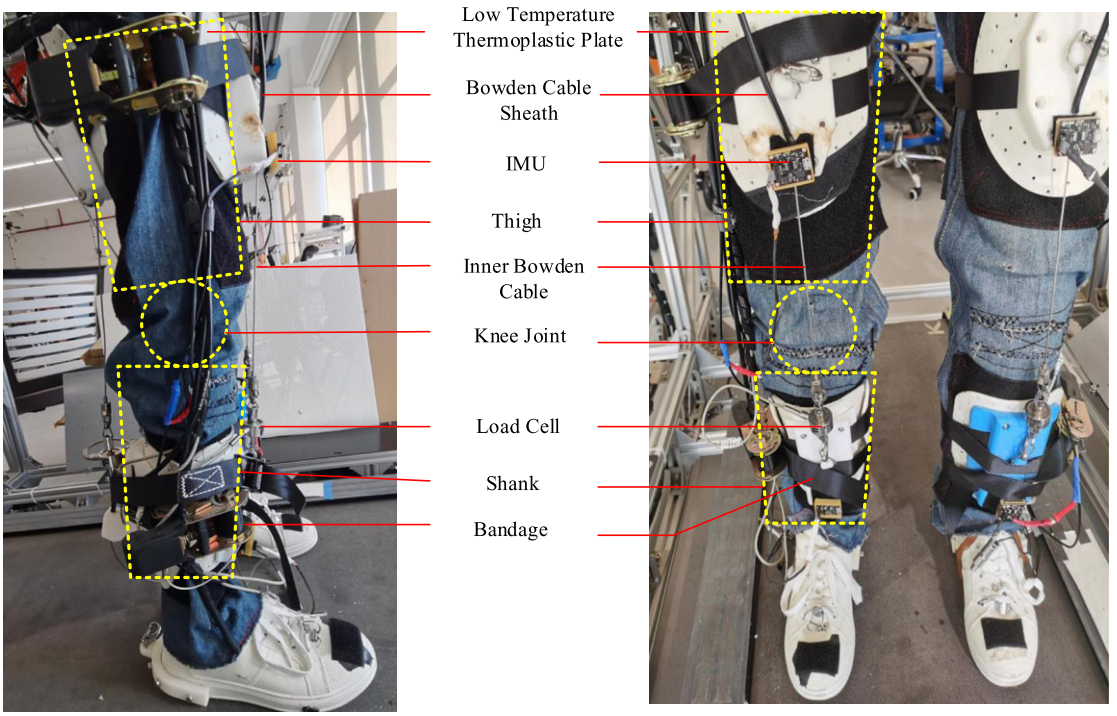


Figure 5. *The prototype of knee exoskeleton in the side view and the front view.*

control performance. The soft property of Bowden cable relates to the comfortability of wearing and using. And it also has a positive relation to the selection of physical size. The suitable diameter of the steel inner cable determines the maximal tensile force. Hence, every parameter exerts an influence on the last performance of the system and needs to be taken into consideration carefully. The main parameters of the Bowden cable in our system is shown in Table II [30].

3.3.1. Driving source and sensor

Consider the knee joint's normal rotation movement (including flexion and extension). In our application, high response speed and precision of motor were selected to meet the requirements of knee joint rotation. Two 180W DC servo motors (EC-i 52, Maxon, Switzerland) for each joint were used to drag the shank movement by Bowden cable. Corresponding parameters in detail about the motor are shown in Table III.

To output the proper torque that exerts on the knee joints, it is indispensable to connect a load cell at the end of an inner steel cable directly. Considering the control need, different force sensors have a crucial influence on system performance. Here the LCM300 (FUTEK, 0∼1500N, USA) load cell was selected, with IAA200 (FUTEK, USA) current transmitter. The total weight of the sensor is 300 g, which is very suitable for a lightweight exoskeleton.

The knee joint angle needs to be monitored when the exoskeleton extern force and torque to the joints. While there is no fixed axis for the exoskeleton to install encoders. The indirect measure approach is more workable for our application. Hence, two inertial measurement units (IMU, LPMS-CURS2, LP-RESEARCH, Japan) have been adopted to sense the posture of the thigh and shank, then by calculating related angle to get the knee joint angle, all the IMUs communicated via the Controller Area Network (CAN) with 1M baud rate.

https://doi.org/10.1017/S0263574722000029 Published online by Cambridge University Press

Table II. *Key parameters of the Bowden cable.*

Parameter	Magnitude
Friction coefficient	0.1
Cable diameter	2 mm
Sheath diameter	6 mm
Max. tension	1500 N

Table III. *Parameters of the servo motor.*

Parameter	Magnitude
Nominal voltage	24 V
Nominal current	6.56A
Nominal speed	4730 rpm
Max. continuous torque	268 mNm
Max. speed	6000 rpm
Max. axial load (dynamic)	30 N
Max. efficiency	88%
Rotor inertia	141 gcm^2
Mechanical time constant	0.654 ms

The control unit is an industrial personal computer (IPC, Beckhoff German) with the EtherCAT communication protocol. The maximum control instruction cycle is 1 ms, which could meet system control demand.

3.3.3. Wearable end actuator

The end wearable actuator is a paramount part that directly reflects the human–machine interaction force. The integrated force from the Bowden cable end should be evenly distributed to the end actuator so that we get a favorable sense of comfort and safety. It must be simple and convenient to put on or off. Therefore, comfort, even distribution of force, and the ability to wear are three major factors that should be considered.

According to ergonomics, the wrapped 3D model that fits the shape contour of tight and shaft was designed. Then, the actuator was made by a low-temperature thermoplastic plate that could be reshaped by the high temperature at 80–100°C. This material not only largely reduces the rubbing and hurting but also fits to lower limbs' surface in certain elastic deformation. The prototype of the knee exoskeleton is shown in Fig. 5.

4. Results and Discussion

From the simulation and the prototype experiments, the method utilized in this paper is correct and feasible, and it is believable that this method is efficient enough to control exoskeleton robots and similar auxiliary equipment. The more detailed information can be explored from the simulation and experiments data.

4.1. Experiments result

Through the simulation, the designed controller based on the dynamics model achieves more favorable performance than conventional PID controller, as shown in Figs. 3 and 4. With the following performance of sine wave trajectory with 0.5 Hz, the proposed controller can make the tracking error close to

https://doi.org/10.1017/S0263574722000029 Published online by Cambridge University Press

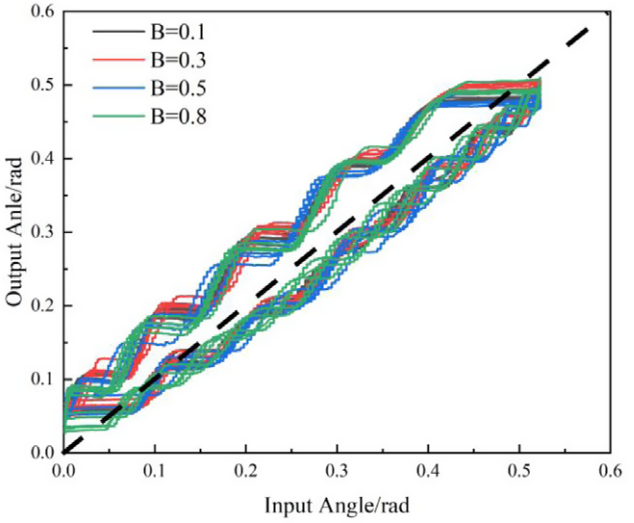


Figure 6. *The characteristic of the Bowden cable transmission system with in difference damping conditions, all of the characteristic curves almost overlapped though there are some hysteresis. The black dash line is 45-degree line.*

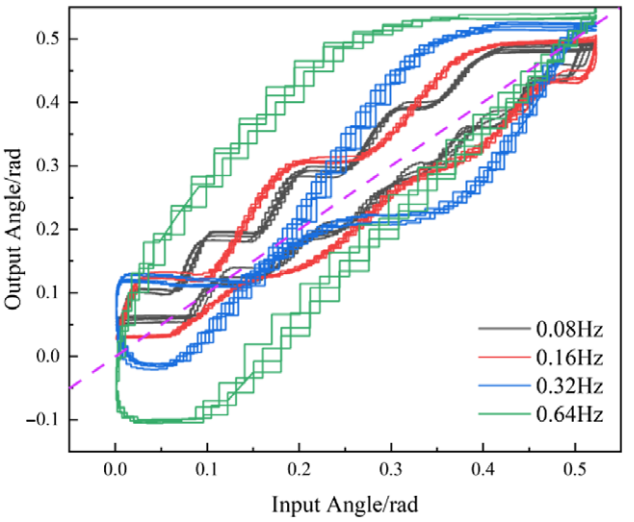


Figure 7. *The input and output characteristic curve with hysteresis. With the frequency increasing, the non-linear degree is more obvious. The pink dash line is 45-degree line.*

zero, while there are always some errors with PID controller. When following the step function, there is less overshot, though they have more response time than the PID controller. It is smoother for the transition process that means the movement is steadier.

According to Fig. 6, it shows the input and output characteristics of the Bowden cable transmission system with the angle in different damping conditions. Most of the curves in different damping parameters overlapped, though there is an obvious hysteresis characteristic, as shown in Fig. 6. In Fig. 7, the nonlinearity of the curves is more obvious with the frequency increasing. In Fig. 8, it shows angular acceleration, angular velocity, and angle variation while tracking the reference joint angle, which is

https://doi.org/10.1017/S0263574722000029 Published online by Cambridge University Press

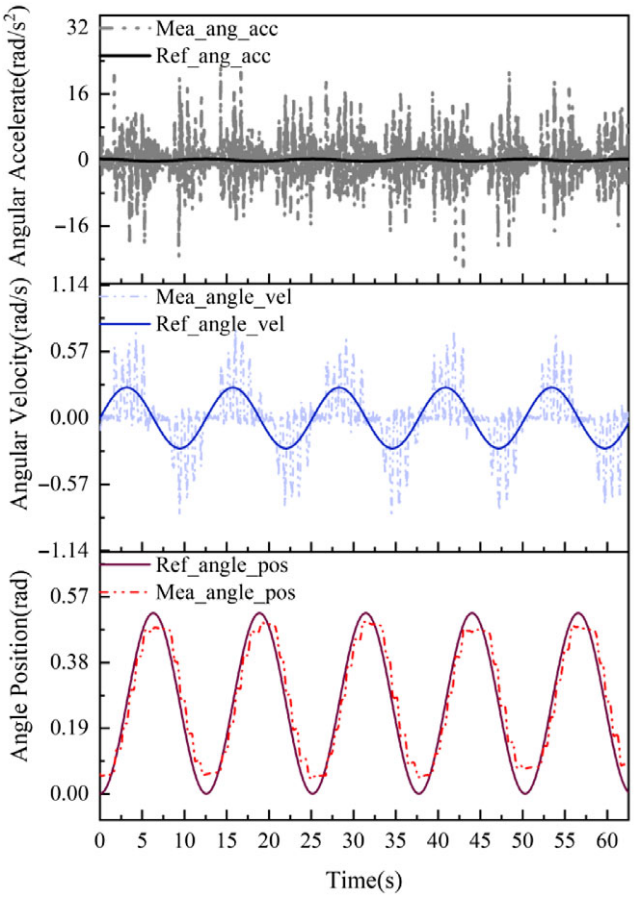


Figure 8. *The knee joint angle (bottom), angular velocity (middle), and angular acceleration (top) variation to follow the reference sine wave (15-degree amplitude and 0.08Hz).*

a sine wave with a 15-degree amplitude at 0.08Hz. The variation of motor output torque, load cells tensions, and the joint torque are shown in Fig. 9 under the same conditions as Fig. 8.

4.2. Discussion

By two Bowden cables exerting force and torque to knee joint, a series of problems coming from rigid exoskeleton can be avoided. Though the mismatch between mechanical and biological joint can be reduced by using double-hinge mechanisms [31], the extra moment of inertia of rigid link and asymmetrical mass attached to the lateral of thigh and shank need to be reduced and limited as much as possible. The two-Bowden cable structure in this paper could avoid aforementioned problems inherently.

As we can see in Fig. 6, different damping condition has been explored to the effect of damping on the transmission process, and the characteristic curve has no obvious changes in different damping parameters. Similarly, it also has no change in the hysteresis characteristic generated from the Bowden cable and motor output. This may be because the angular velocity is low, which the damping item is small on the control torque output.

The different frequencies of the input signal exert more influence on the output, as shown in Fig. 7. The faster of signals are, the more non-linear and hysteresis have been performed. This may be due to the fact that the response characteristics of the Bowden cable determine the output characteristics of the

https://doi.org/10.1017/S0263574722000029 Published online by Cambridge University Press

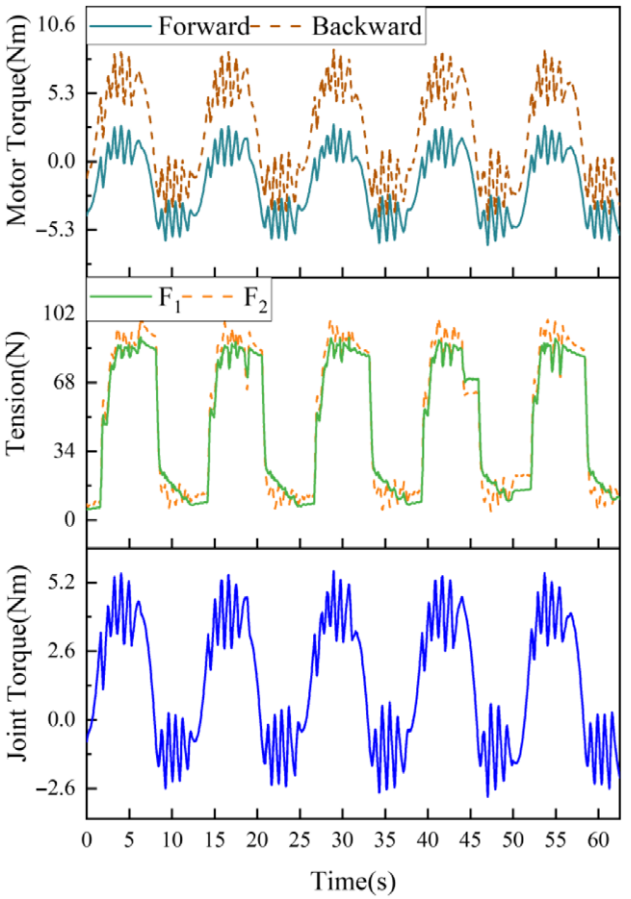


Figure 9. *The joint torque (bottom), tension (middle), and motor output torque (top) variation with the time when the exoskeleton assisted the knee joint to track the reference sine wave (15-degree amplitude and 0.08 Hz).*

model, which is a problem that many previous studies [32, 33] have also encountered. Hence, it should consider the signal frequency when the Bowden cable system has been utilized to the transmission system with continuously changing requirements.

In Fig. 8, the exoskeleton joint (bottom figure in Fig. 8) basically tracked the reference angle trajectory. And the velocity is general consistency considering the real velocity calculated by the numerical difference method (middle figure in Fig. 8). There is no obvious relationship between reference angular acceleration and measure angular one (top figure in Fig. 8). This may be because the numerical difference introduced significant error according to measuring angular velocity. Hence, a more accurate measurement method may need to measure the angular velocity to avoid enormous error and noise. Compared to the simulation in Fig. 3, the angle error rapidly convergence to zero, and the experience seems to have some space to improve in tracking errors. Namely, more real factors, such as friction, hysteresis, and dead zone, of driving and transmission systems may need to be weighed.

Motion comes from the action of joint moments. It is also important to analyze the effect of the exoskeleton on the improvement of joint torque and joint range of motion [34]. The desired motion in Fig. 8 is driven by torque and force shown in Fig. 9. The bottom figure shows the joint's torque according to real-time status, the middle figure shows the Bowden cable tension. And the top figure is the motors' real torque output, which is calculated according to the model mentioned in Part II Methodology. There

https://doi.org/10.1017/S0263574722000029 Published online by Cambridge University Press

is a shake in peak, and the corresponding angle curve has distortion in corresponding time in Fig. 8. This may be because of the Bowden cable limit shank to tracking reference value, but the output torque is still adjusted according to the state variable. The main antagonistic motion also takes place at this moment according to the tension variation figure in Fig. 8 (middle figure).

The reliability of the device is also very important, in order to verify the reliable performance of the device under different parameters [35]. In this article, the operation of the knee joint with different frequencies and damping parameters in several attempts to verify the reliability of the exoskeleton. Compared Fig. 3 with Fig. 8, the control method in ideal conditions may deteriorate in reality because plenty of uncertain factors, such as friction and hysteresis, play a role in practice. Though the simulation results are consistent with the real experiments in the aspect of system stability, there are some differences in both. Simulation is a wonderful method to verify the feasibility, but real experiments apparently take a more crucial role in controlling the actual system. Compared Fig. 7 with Fig. 8, the results of the tests under different damping and frequency conditions show that the exoskeleton works reliably under the conditions tested, although different model parameters affect the actual performance of the exoskeleton. In all, all experiments were able to be performed normally, and the knee joint exoskeleton showed a considerable reliability.

5. Conclusion and Expectation

5.1. Conclusion

According to the results and analysis of the concrete experiment, we can draw the conclusion safely that the method proposed in the paper is correct and feasible. The control stability of the exoskeleton system has been proven. And this method can achieve a favorable control performance with the knee joint rehabilitation exoskeleton robot.

5.2. Future work

In the future, more research should be done about the relationship between biomechanism of the body and exoskeleton robot. This relationship can exert an immense influence on the safety, comfort, and the performance. Multi-joints exoskeleton robots also need be developed to assist with more limb joints, so that poststroke patients can get comprehensive and multi-stage treatment.

Conflicts of Interest

None.

Financial Support

This work was supported in part by the National Natural Science Foundation of China (Grant No. 52075177), Joint Fund of the Ministry of Education for Equipment Pre-Research (Grant No. 6141A02033124), Research Foundation of Guangdong Province (Grant No. 2019A050505001 and 2018KZDXM002), and Guangzhou Research Foundation (Grant No. 202002030324 and 201903010028).

Ethical Considerations

None.

https://doi.org/10.1017/S0263574722000029 Published online by Cambridge University Press

Authors' Contributions

None.

References

[1] M. Zhou, H. Wang, X. Zeng, P. Yin, J. Zhu, W. Chen, X. Li, L. Wang, L. Wang and Y. J. T. L. Liu, "Mortality, morbidity, and risk factors in China and its provinces, 1990–2017: a systematic analysis for the Global Burden of Disease Study 2017," *The Lancet.* **394**(10204), 1145–1158 (2019)..

[2] J. S. Sulzer, R. A. Roiz, M. A. Peshkin and J. L. Patton, "A highly backdrivable, lightweight knee actuator for investigating gait in stroke," *IEEE Trans. Rob.* **25**(3), 539–548 (2009).

[3] D. Park, H. In, H. Lee, S. Lee, I. Koo, B. B. Kang, K. Park, W. S. Chang and K.-J. Cho, "Preliminary study for a soft wearable knee extensor to assist physically weak people," *2014 11th International Conference on Ubiquitous Robots and Ambient Intelligence (URAI).* pp. 136–137.

[4] K. Schmidt, J. E. Duarte, M. Grimmer, A. Sancho-Puchades, H. Wei, C. S. Easthope and R. Riener, "The myosuit: Bi-articular anti-gravity exosuit that reduces hip extensor activity in sitting transfers," *Front. Neurorob.* **11**, 57 (2017).

[5] S. H. Collins, M. B. Wiggin and G. S. Sawicki, "Reducing the energy cost of human walking using an unpowered exoskeleton," *Nature.* **522**(7555), 212–215 (2015).

[6] S. J. Phee, S. C. Low, P. Dario and A. Menciassi, "Tendon sheath analysis for estimation of distal end force and elongation for sensorless distal end," *Robotica*. **28**(7), 1073–1082 (2010).

[7] S. S. Cheng, X. Wang and J. P. Desai, "Design and analysis of a remotely-actuated cable-driven neurosurgical robot." *2017 IEEE/RSJ International Conference on Intelligent Robots and Systems (IROS). IEEE.* pp. 1685–1690.

[8] B. K. Dinh, M. Xiloyannis, C. W. Antuvan, L. Cappello and L. Masia, "Hierarchical cascade controller for assistance modulation in a soft wearable arm exoskeleton," *IEEE Robot. Autom. Lett.* **2**(3), 1786–1793 (2017).

[9] J.-Y. Kuan, K. A. Pasch and H. M. Herr, "A high-performance cable-drive module for the development of wearable devices," *IEEE/ASME Trans. Mechatron.* **23**(3), 1238–1248 (2018).

[10] L. N. Awad, J. Bae, K. O'donnell, S. M. De Rossi, K. Hendron, L. H. Sloot, P. Kudzia, S. Allen, K. G. Holt and T. D. Ellis, "A soft robotic exosuit improves walking in patients after stroke," *Sci. Transl. Med.* **9**(400), eaai9084 (2017).

[11] P. Malcolm, S. Lee, S. Crea, C. Siviy, F. Saucedo, I. Galiana, F. A. Panizzolo, K. G. Holt and C. J. Walsh, "Varying negative work assistance at the ankle with a soft exosuit during loaded walking," *J. Neuroeng. Rehabil.* **14**(1), 62 (2017).

[12] Y. Ding, I. Galiana, C. Siviy, F. A. Panizzolo and C. Walsh, "IMU-based iterative control for hip extension assistance with a soft exosuit." *2016 IEEE International Conference on Robotics and Automation (ICRA). IEEE.* pp. 3501–3508.

[13] Y. M. Senturk, and V. Patoglu, "MRI-VisAct: a Bowden-cable-driven MRI-compatible series viscoelastic actuator," *Trans. Inst. Meas. Control.* **40**(8), 2440–2453 (2018).

[14] I. Gaponov and J.-H. Ryu, "Twisted String Actuators: Life Cycle, Twisting inside Bowden Cables, and Passive Return Mechanisms," *Stroke*. **10**, 20 (2016).

[15] N. Thompson, A. Sinha and G. Krishnan, "Characterizing architectures of soft pneumatic actuators for a cable-driven shoulder exoskeleton." *2019 International Conference on Robotics and Automation (ICRA).* pp. 570–576.

[16] Y. Ding, M. Kim, S. Kuindersma and C. J. Walsh, "Human-in-the-loop optimization of hip assistance with a soft exosuit during walking," *Sci. Robot.* **3**(15), eaar5438 (2018).

[17] J. Zhang, P. Fiers, K. A. Witte, R. W. Jackson, K. L. Poggensee, C. G. Atkeson and S. H. Collins, "Human-in-the-loop optimization of exoskeleton assistance during walking," *Science.* **356**(6344), 1280–1284 (2017).

[18] Y. Ding, F. A. Panizzolo, C. Siviy, P. Malcolm, I. Galiana, K. G. Holt and C. J. Walsh, "Effect of timing of hip extension assistance during loaded walking with a soft exosuit," *J. Neuroeng. Rehabil.* **13**(1), 87 (2016).

[19] F. A. Panizzolo, I. Galiana, A. T. Asbeck, C. Siviy, K. Schmidt, K. G. Holt and C. J. Walsh, "A biologically-inspired multi-joint soft exosuit that can reduce the energy cost of loaded walking," *J. Neuroeng. Rehabil.* **13**(1), 43 (2016).

[20] B. Quinlivan, S. Lee, P. Malcolm, D. Rossi, M. Grimmer, C. Siviy, N. Karavas, D. Wagner, A. Asbeck and I. Galiana, "Assistance magnitude versus metabolic cost reductions for a tethered multiarticular soft exosuit," *Sci. Robot.* **2**(2), 1–10 (2017).

[21] U. Jeong and K.-J. Cho, "A feasibility study on tension control of Bowden-cable based on a dual-wire scheme." *2017 IEEE international conference on robotics and automation (ICRA). IEEE.* pp. 3690–3695.

[22] J. F. Rodríguez-León, B. D. Chaparro-Rico, M. Russo and D. Cafolla, "An Autotuning Cable-Driven Device for Home Rehabilitation," *J. Healthcare Eng*. **2021** (2021).

[23] J. Hamill and K. M. Knutzen, *Biomechanical basis of human movement* (Lippincott Williams & Wilkins, 2006).

[24] J. Musić, R. Kamnik, V. Zanchi and M. Munih, "Human body model based inertial measurement of sit-to-stand motion kinematics," *WSEAS Trans. Syst*. **7**(3), 156–164 (2008).

[25] C. Yang, Q. Huang, Z. Ye and J. Han, "Dynamic modeling of spatial 6-DOF parallel robots using Kane method for control purposes." *2010 Second International Conference on Intelligent Human-Machine Systems and Cybernetics.* pp. 180–183.

[26] P. R. Vundavilli and D. K. Pratihar, "Dynamically Balanced Ascending Gait Generation of a Biped Robot Negotiating Staircase." *2008 IEEE Region 10 and the Third international Conference on Industrial and Information Systems. IEEE.* pp. 1–6.

[27] D. A. Winter, *Biomechanics and motor control of human movement* (John Wiley & Sons, 2009).

https://doi.org/10.1017/S0263574722000029 Published online by Cambridge University Press

[28] Y. Hong and R. Bartlett, *Routledge handbook of biomechanics and human movement science* (Routledge, 2008).
[29] G. E. Robertson, G. E. Caldwell, J. Hamill, G. Kamen and S. Whittlesey, *Research methods in biomechanics* (Human kinetics, 2013).
[30] M. Kaneko, T. Yamashita and K. Tanie, "Basic considerations on transmission characteristics for tendon drive robots." *Fifth International Conference on Advanced Robotics' Robots in Unstructured Environments. IEEE.* pp. 827–832.
[31] J. Wang, X. Li, T.-H. Huang, S. Yu, Y. Li, T. Chen, A. Carriero, M. Oh-Park, H. J. I. R. Su and A. Letters, "Comfort-centered design of a lightweight and backdrivable knee exoskeleton," *IEEE Robotics and Automation Letters.* **3**(4), 4265–4272 (2018).
[32] F. Zhang, L. Yang and Y. Fu, "Design of a novel elastic torque sensor for hand injuries rehabilitation based on bowden cable," *IEEE Trans. Instrum. Meas.* **68**(9), 3184–3192 (2018).
[33] M. Yin, H. Wu, Z. Xu, W. Han and Z. Zhao, "Compliant control of single tendon-sheath actuators applied to a robotic manipulator," *IEEE Access.* **8**, 37361–37371 (2020).
[34] B. D. Chaparro-Rico, D. Cafolla, P. Tortola and G. J. A. S. Galardi, "Assessing Stiffness, Joint Torque and ROM for Paretic and Non-Paretic Lower Limbs during the Subacute Phase of Stroke Using Lokomat Tools," *Appl. Sci.* **10**(18), 6168 (2020).
[35] B. D. Chaparro-Rico and D. J. A. S. Cafolla, "Test-retest, inter-rater and intra-rater reliability for spatiotemporal gait parameters using SANE (an eaSy gAit aNalysis systEm) as measuring instrument," *Appl. Sci.* **10**(17), 5781 (2020).

Cite this article: B. Liu, YW. Liu, Z. Zhou and L. Xie (2022). "Control of flexible knee joint exoskeleton robot based on dynamic model", Robotica **40**, 2996–3012. https://doi.org/10.1017/S0263574722000029

https://doi.org/10.1017/S0263574722000029 Published online by Cambridge University Press